Journal of Applied Mathematics and Physics (ZAMP)
Vol. 39, January 1988

0044-2275/88/001013-15 $ 4.50/0

Low-Reynolds-number modelling of flows over a backward-facing step

By R. M. C. So, Y. G. Lai, Mechanical and Aerospace Engineering, Arizona State University, Tempe, AZ 85287, B. C. Hwang, David Taylor Naval Ship Research & Development Center, Annapolis, MD 21402, and G. J. Yoo, Mechanical and Aerospace Engineering, Arizona State University, Tempe, AZ 85287, USA

1. Introduction

According to Bradshaw and Wong [1], the flow of a thin boundary layer over a backward-facing step involves two "overwhelming" perturbations. The first is the perturbation of a boundary layer into a mixing layer and the second is the conversion of the attached mixing layer back to a boundary layer. As a result of these perturbations, the flow behind the backward-facing step becomes very complicated and embodies a wide variety of complex turbulent flows. For example, it involves streamline curvature because the new mixing layer is curved toward the wall to form a recirculation region (Fig. 1). The new mixing layer bifurcates at the reattachment point with one branch develops as a new boundary layer after the reattachment point and the other branch forms the recirculation region. Therefore, the flow undergoes rapid distortion in the region surrounding the reattachment point and subsequent relaxation downstream of this point. It is precisely because of these complexities that the flow becomes a classic example for researchers to model and calculate. If a turbulence model can reproduce this flow correctly, then the possibilities that the model is equally successful with other types of turbulent flow are greatly increased.

Various boundary-layer calculation methods have been developed to calculate this flow [2]. However, they are not very successful in the prediction of the recovery region downstream of the reattachment point. The main reason is that the turbulence length scale downstream of the reattachment point is closely related to that in the mixing layer before reattachment and is substantially larger than that in a turbulent boundary layer determined from local-equilibrium arguments [1, 3]. This implies that the near-wall turbulence length scale ℓ is no longer given by $\ell = \kappa y$, where $\kappa = 0.42$ is the von Karman constant and y is the normal coordinate measured from the wall. Instaed, $\ell = Ky$, where $K \cong 1$

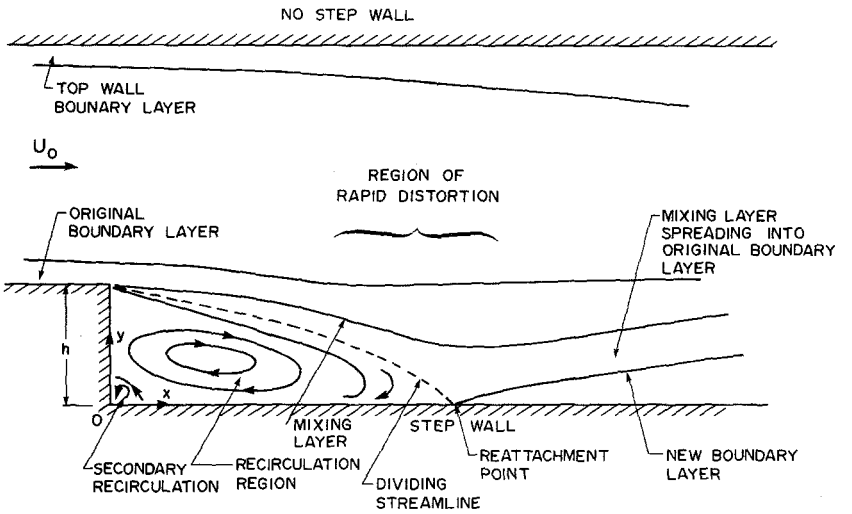

Figure 1
Pictorial representation of flow over a backward-facing step.

[3]. Therefore, boundary-layer methods based on local-equilibrium arguments are inadequate.

Numerous elliptic methods, where the Reynolds equations of motion are solved rather than the boundary-layer equations, have also been proposed [2, 4–6]. The turbulence closures proposed range from simple mixing-length models to full Reynolds stress models, where the transport equations of the Reynolds stresses are solved simultaneously with the Reynolds equations of motion. In the case of mixing-length models, the assumption, $\ell = \kappa y D$, is invariably invoked, where D is the van Driest damping factor used to account for viscous effects near a wall. As for the other models, the closure assumptions are based on high-Reynolds-number turbulence arguments and are not applicable near a wall [4–6]. Consequently, near-wall flow models or wall functions have to be proposed in order to link the flow at the wall to the flow in the fully turbulent region away from the wall. Different wall functions have been tried [4, 6]. However, they are essentially based on the local-equilibrium arguments. Some typical examples of the application of these methods to calculate flows over a backward-facing step are provided by Sindir [5] and Celenligil and Mellor [6]. Four closure models are examined by Sindir [5] and these are the $k - \varepsilon$ and algebraic stress models and their modifications to account for streamline curvature. Only the modified algebraic stress model is found to give good agreement with the data of Kim et al. [7], including the skin friction (c_f) prediction in the recovery region downstream of the reattachment point. On the other hand, Celenligil and Mellor [6] solve the unsteady governing equations and model the flow with a full Reynolds stress closure. Their calculations are in good agreement with the measurements of Kim et al. [7] and Westphal et al. [8].

Up to now, no attempts have been made to calculate the flow without invoking the conventional wall function assumption. Since the flow downstream of a backward-facing step embodies a wide variety of complex turbulent shear flows (Fig. 1), the nearwall turbulent flow may not be in local equilibrium. This is especially true of the flow in the vicinity of the reattachment point, where viscous effects are dominant. Consequently, the wall function assumption for near-wall flow may not be applicable. The present objective is to evaluate the validity and extent of the wall function assumption for the calculation of flow over a backward-facing step. This is accomplished by developing a low-Reynolds-number turbulence model for the flow behind a backward-facing step where the calculation is carried out directly to the wall. The model is verified by comparing the calculations with measurements and the validity and extent of the wall function assumption is assessed by a detailed comparison of the two models' performance with experimental data.

A good review of two-dimensional sudden-expansion flows up to 1980 is given by Eaton and Johnston [9]. Since then, detailed velocity measurements of flow over a backward-facing step using laser Doppler techniques are available. A good example of these measurements is provided by Stevenson et al. [10]. However, most of these experiments do not include data on c_f and the velocity measurements are not made close enough to the wall to allow c_f to be interpreted from the velocity gradient at the wall. Consequently, they cannot be used to validate the turbulence model applied to calculate c_f. The two experiments that provide c_f measurements are those given by [1] and [8]. Since the detailed velocity field measurements of [8] are reported in [9], the present calculations are compared with the measurements of [1], [8] and [9].

2. The governing equations

For stationary, incompressible, isothermal turbulent flow over a backward-facing step, the governing Reynolds equations can be concisely written in Cartesian tensor notation as

$$\frac{\partial U_i}{\partial x_i} = 0 \,, \tag{1}$$

$$U_j \frac{\partial U_i}{\partial x_j} = -\frac{1}{\varrho}\frac{\partial P}{\partial x_i} + \frac{\partial}{\partial x_j}\left(\nu \frac{\partial U_i}{\partial x_j} - \overline{u_i u_j}\right) \,, \tag{2}$$

where U_j and u_j are the j^{th} components of the mean and fluctuating velocity, respectively, P is the mean pressure, ϱ and ν are the fluid density and kinematic viscosity and x_j is the j^{th} component of the coordinates. The transport of $\overline{u_i u_j}$

is given by the Reynolds stress equations, which can be written symbolically as [11]:

$$U_k \frac{\partial \overline{u_i u_j}}{\partial x_k} = \boldsymbol{D}_{ij}^v + \boldsymbol{D}_{ij}^T + P_{ij} + \Phi_{ij} - \varepsilon_{ij} \ , \tag{3}$$

where $\boldsymbol{D}_{ij}^v$ *and* $\boldsymbol{D}_{ij}^T$ represent the viscous and turbulent diffusion of $\overline{u_i u_j}$, respectively, P_{ij} is the reproduction of $\overline{u_i u_j}$ by mean shear, Φ_{ij} is the redistribution of $\overline{u_i u_j}$ by the fluctuating pressure and ε_{ij} is the dissipation of $\overline{u_i u_j}$ by viscosity. Of the five terms on the RHS of (3), only $\boldsymbol{D}_{ij}^v$ and P_{ij} are expressible in terms of $\overline{u_i u_j}$ and $\partial U_i / \partial x_j$. The others either involve higher-order correlation of u_i, correlations with the fluctuating pressure p or correlations with the gradient of u_i. If Eqs. (1)–(3) are to form a closed set of equations for U_i, P and $\overline{u_i u_j}$, then turbulence models have to be proposed for $\boldsymbol{D}_{ij}^T$, Φ_{ij} and ε_{ij}. The present study attempts to solve (1)–(3) with appropriate models for $\boldsymbol{D}_{ij}^T$, Φ_{ij} and ε_{ij} for the flow over a backward-facing step.

3. The turbulence closures

Conventional full Reynolds stress closures are developed for high-Reynolds-number turbulence, while a wall function approximation is applied to the region very close to the wall. Therefore, in actual computations, the first grid point is located outside the viscous wall layer so that the high-Reynolds-number closure is valid and the wall function [4] is used to link the conditions at the wall to the first grid point. A typical example of such a closure is that due to Launder et al. [11]. In this closure, $\boldsymbol{D}_{ij}^v$ is neglected while $\boldsymbol{D}_{ij}^T$ is modelled according to the suggestion of Hanjalic and Launder [12], Φ_{ij} is modelled with mean-strain effects [11] and ε_{ij} is given by the locally isotropic model of Kolmogorov [13]. There are numerous other full Reynolds stress closures. Some are tailored to model a particular type of flow; for example [14] where the model for Φ_{ij} is modified to account for streamline curvature and swirl effects. In spite of this development, little advance has been made toward the development of a low-Reynolds-number full Reynolds stress closure for complex turbulent flows.

Recently, two low-Reynolds-number full Reynolds stress closures are put forward and validated against periodic flows [15] and shear flows [16]. The two models are quite similar, in that they only modify the model for ε_{ij} to account for viscous effects near a wall and retain $\boldsymbol{D}_{ij}^v$ in (3) and the conventional high-Reynolds-number models for Φ_{ij} and $\boldsymbol{D}_{ij}^T$. A comparison of the performance of these two closures has also been made by So and Yoo [16] and they find that, if the models for $\boldsymbol{D}_{ij}^T$ and Φ_{ij} are maintained the same, the two ε_{ij} models give essentially the same predictions of wall shear flows. Later, So and Yoo [17] apply the model of [16] to calculate shear flow with wall transpiration and find good

agreement with measurement, while the conventional wall function approach gives results that are at variance with the measured wall pressure distribution.

The calculations of [11] and [14] show that the modelling of Φ_{ij} is fairly important to the overall predicitions depending on the type of turbulent flows considered, while the results are not too dependent on the models for $\boldsymbol{D}_{ij}^{T}$. Therefore, it is clear that, for the present investigation, the effects of Φ_{ij} modelling have to be examined in addition to the effects of near-wall flow modelling. In view of this, three different Φ_{ij} models are investigated. These are the models of Rotta [18], Gibson and Younis [14] and Launder et al. [11]. Two near-wall flow models are studied. These are the wall function approximation [4] and the low-Reynolds-number model of So and Yoo [16]. A summary and labelling of these different closures is given in Table 1.

Table 1
Labelling of different turbulence closures.

Closure	$\boldsymbol{D}_{ij}^{T}$	Φ_{ij}			ε_{ij}		Wall function assumption
	Hanjalic and Launder [12]	Rotta [18]	Launder, Reece and Rodi [11]	Gibson and Younis [14]	So and Yoo [16]	Kolmogorov [13]	
A1	X	X	–	–	X	–	NO
A2	X	–	X	–	X	–	NO
A4	X	–	–	X	X	–	NO
H–A1	X	X	–	–	–	X	YES

The modelling of $\boldsymbol{D}_{ij}^{T}$, Φ_{ij} and ε_{ij} introduces yet another unknown; namely, the dissipation rate ε of the turbulent kinetic energy k. Consequently, an additional equation governing the transport of ε is required. Consistent with the approach of [16], the modified ε equation of Chien [19] is used. This can be written as:

$$U_k \frac{\partial \varepsilon}{\partial x_k} = \frac{\partial}{\partial x_k}\left[\left(\nu + \frac{\nu_t}{\sigma_\varepsilon}\right)\frac{\partial \varepsilon}{\partial x_k}\right] + C_{\varepsilon 1}\frac{\varepsilon}{k}\tilde{P} - C_{\varepsilon 2} f_1 \frac{\varepsilon^2}{k} - \frac{2\nu\varepsilon}{x_2^2} e^{-C_4 x_2 u_\tau/\nu}, \tag{4}$$

where
$$\tilde{P} = -\overline{u_i u_k}\frac{\partial U_i}{\partial x_k},$$
$$\nu_t = C_\mu \frac{k^2}{\varepsilon} f_2,$$
$$f_1 = 1 - \frac{2}{9} e^{-(k^2/6\nu\varepsilon)^2}, \tag{5}$$
$$f_2 = 1 - e^{-C_3 u_\tau x_2/\nu},$$

x_2 is the normal coordinate measured from the wall, $u_\tau = U_0 (c_f/2)^{1/2}$ is the wall friction velocity, U_0 is the uniform inlet velocity and σ_ε, $C_{\varepsilon 1}$, $C_{\varepsilon 2}$, C_μ, C_3 and C_4 are model constants. The values of these and other model constants introduced through D_{ij}^T, Φ_{ij} and ε_{ij} are given in [14] and [16] and are used in the present calculations without change.

Finally, a low-Reynolds-number $k - \varepsilon$ closure, designated as $L - k - \varepsilon$, is also investigated and its performance compared with the full Reynolds stress closures. The $L - k - \varepsilon$ chosen is the one proposed by Chien [19]. Therefore, altogether four low-Reynolds-number and one high-Reynolds-number closures are used to calculate the backward-facing step flow.

4. Solution technique

The boundary conditions for the backward-facing step flow are no slip conditions at both the step and no step walls. All turbulence quantities, $\overline{u_i u_j}$ and ε, are taken to be zero at the walls. At the inlet, experimentally specified conditions are used while at the outlet, the condition $\partial \Psi / \partial x = 0$ is invoked, where Ψ is any flow variable except pressure and x is the stream coordinate measured from the step.

The coupled Eqs. (1)–(4) and boundary conditions are solved numerically using either hybrid or quadratic upwind finite differencing and staggered grids. A fixed pressure field is assumed and the momentum equations are solved iteratively using the SIMPLE algorithm of Patankar and Spalding [20]. After each sweep over the solution domain, adjustments are made to the pressure field to satisfy continuity along each line of cells. Transport equations for $\overline{u_i u_j}$ and ε are then solved using the calculated velocity field. Iterations are carried out until the momentum and continuity equations are simultaneously satisfied. An accuracy criterion of relative mass and velocity residuals $\leqq 1\,\%$ is stipulated.

5. Choice of grids

Non-uniform computational grids are used to resolve the flow in the region of interest. Previously, So and Yoo [16] have examined the effect of grid spacing in the normal or y-direction on the near-wall flow calculations. They found that a minimum of 10 grid points are required between the wall ($y = 0$) and the grid point just outside the viscous sublayer. For more complicated near-wall flows, up to 15 grid points are necessary to resolve the flow in this region. Based on this guideline, 15 grid points are specified near the step wall and 10 grid points are specified near the top or no step wall. Consequently, the low-Reynolds-number calculations are carried out with 66 grid points specified in the y-direction. This is reduced to 41 points for the high-Reynolds-number closure. As for grid

spacing in the stream or x-direction, a numerical experiment is carried out to determine the effect of grid spacing on the calculated flow properties. The calculations are carried out over the backward-facing step geometry of [9] and assuming the flow to be laminar. Three different inlet flow Reynolds numbers ($\mathrm{Re} = U_0 W/\nu$ where W is the inlet width) are specified and these are Re = 200, 500 and 1000, respectively. Also, three different grids are tested; these are given by 50 × 66, 78 × 66 and 93 × 66. Therefore, the y-direction grid spacings are kept constant, while the x-direction grid spacings are varied from 50 to 93. The results, shown with U, the stream velocity, normalized by the maximum stream velocity, $U_{\max}$, for the case Re = 500 are plotted in Fig. 2. It can bee seen that the U velocity is grid independent when the number of grid points in the x-direction is $\geqq 78$. Identical results are also obtained for the Re = 200 and 1000 cases. Therefore, the flow over a backward-facing step should be carried out with a grid of 78 × 66. The layout of this grid is shown in Fig. 3.

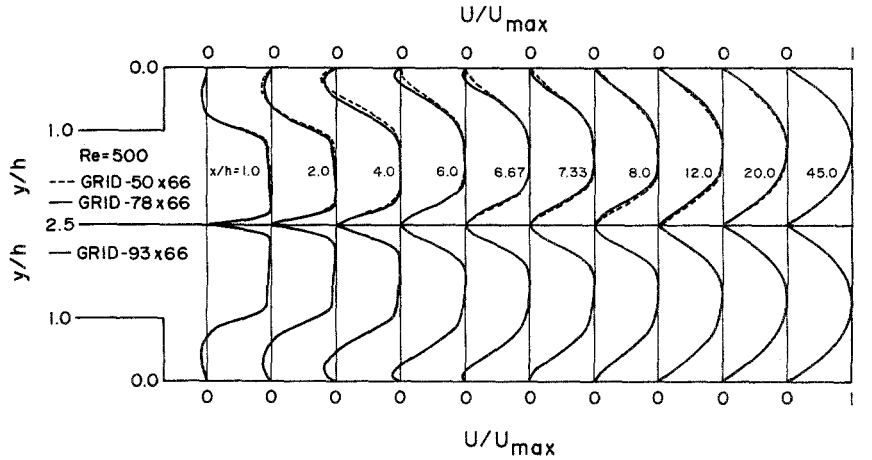

Figure 2
Comparison of calculated $U/U_{\max}$ using different grids for laminar flow over a backward-facing step.

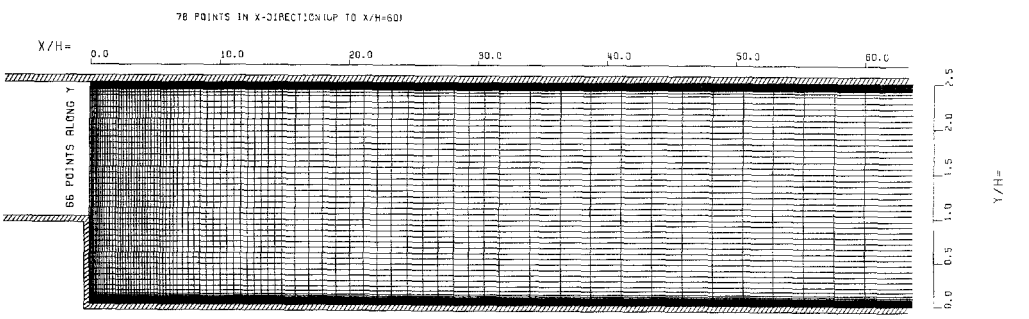

Figure 3
Layout of the grid used for present calculations.

6. Discussion of results

The primary objective of the present study is to develop and validate a low-Reynolds-number turbulence model for the flow behind a backward-facing step. This means that the model should be able to describe the flow in both the recirculation region and the relaxing flow downstream of the reattachment point, x_r. Besides, the present study also addresses the question of Φ_{ij} modelling and its importance in the prediction of the overall behavior in complex turbulent flows.

Calculations of the backward-facing step flows [1], [8] and [9] are carried out with the closures listed in Table 1 plus the $L - k - \varepsilon$ closure. All the calculations are carried out with the grid shown in Fig. 3. Comparison with the data of [9] are shown in Figs. 4–7 and organized in the following manner. Each plot is divided into a top and a bottom part and each part shows the complete backward-facing step geometry. The coordinates x, y are normalized with respect to the step height h, and the velocity data are normalized with respect to the uniform inlet velocity U_0. Each part shows the comparison of two closure calculations with data; A1 and A2 are shown on the top while H–A1 and A4 are shown on the bottom. This presentation allows the differences between various closures to be clearly displayed. The $L - k - \varepsilon$ mean and turbulence field calculations are poor compared to measurements and other closure results. Therefore, they are not shown in Figs. 4–7 for comparison. However, the $L - k - \varepsilon$ results for x_r and c_f are comparable to other low-Reynolds-number model calculations and are also shown in Figs. 8 and 9 for comparison. A sample stream function plot is shown in Fig. 10. Finally, a comparison of the calculated c_f behavior downstream of the reattachment point with measurements [1, 8] are presented in Fig. 11, and a comparison of the pressure distribution, $C_p - (C_p)_{\min}$, on both walls is shown in Fig. 12, where C_p is the pressure coefficient defined with respect to U_0.

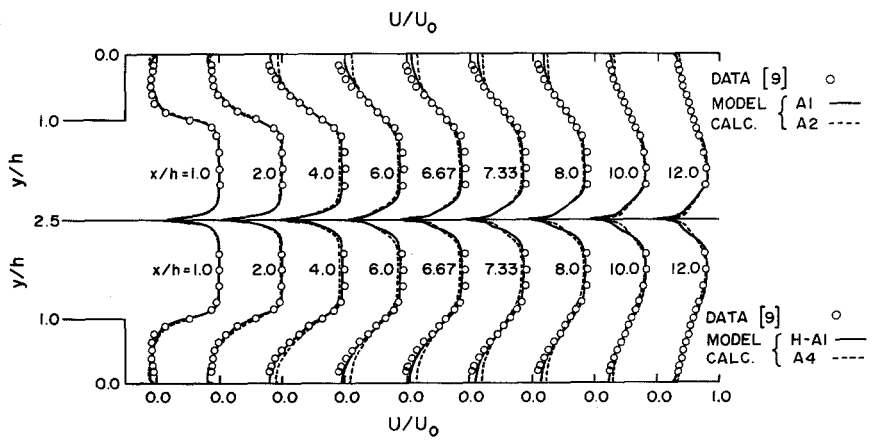

Figure 4
Comparison of the calculated and measured mean velocity.

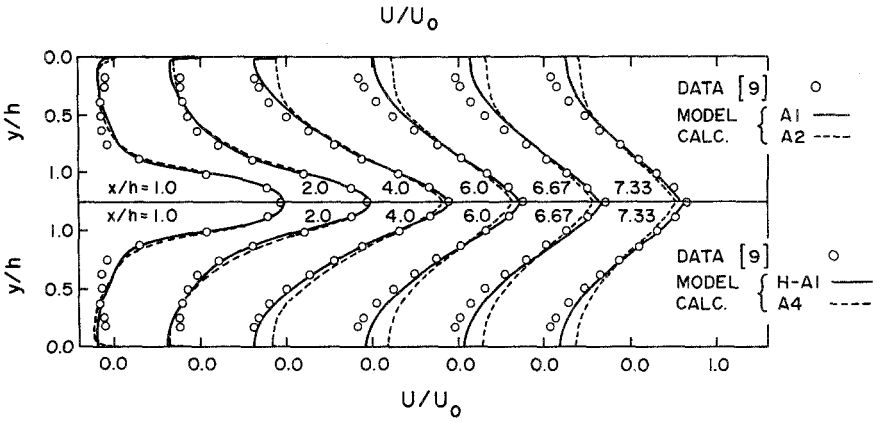

Figure 5
Comparison of the calculated and measured U in the recirculation region.

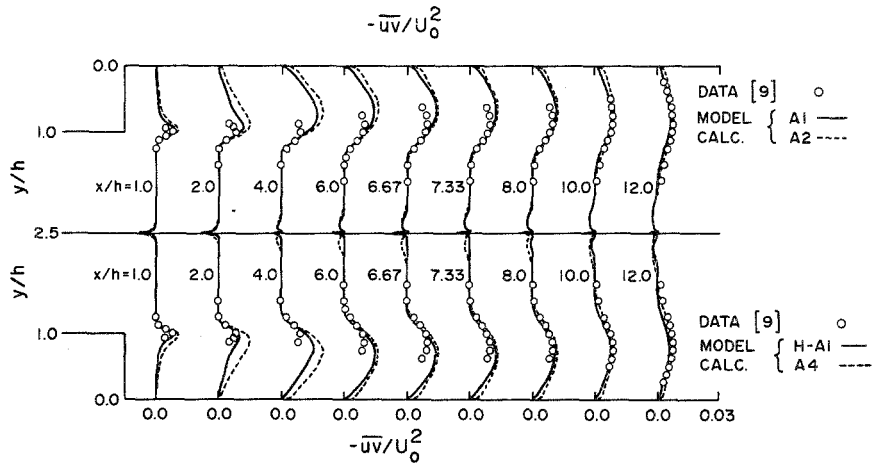

Figure 6
Comparison of the calculated and measured $\overline{uv}$.

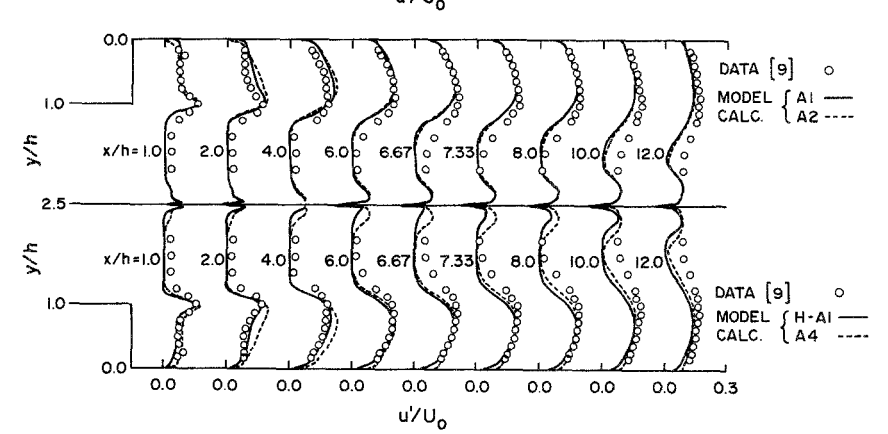

Figure 7
Comparison of the calculated and measured u'.

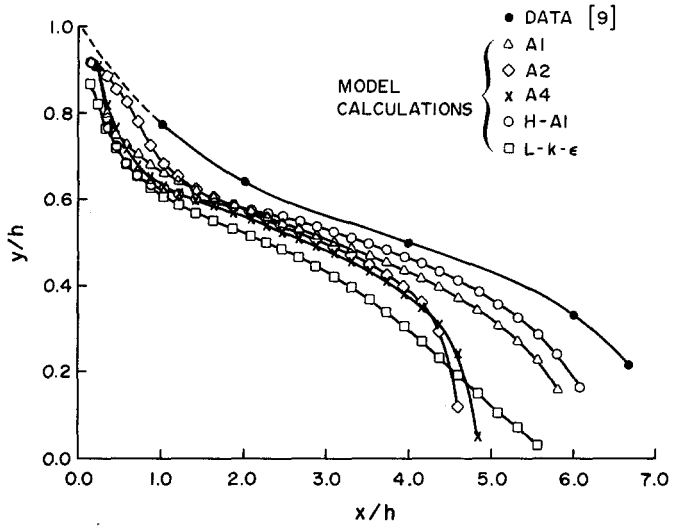

Figure 8
Comparison of the calculated and measured $U = 0$ locus.

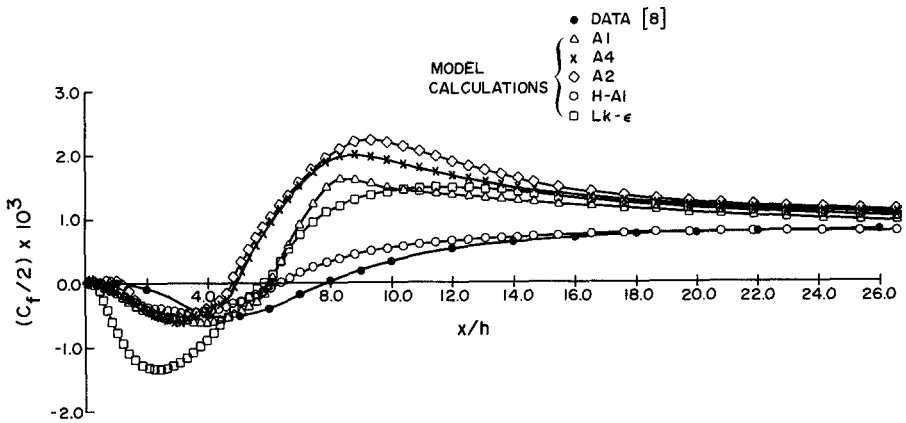

Figure 9
Comparison of the calculated and measured c_f.

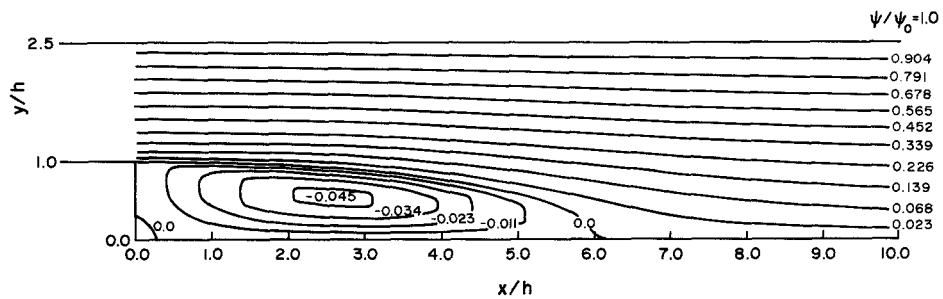

Figure 10
A plot of the normalized stream function ψ/ψ_0.

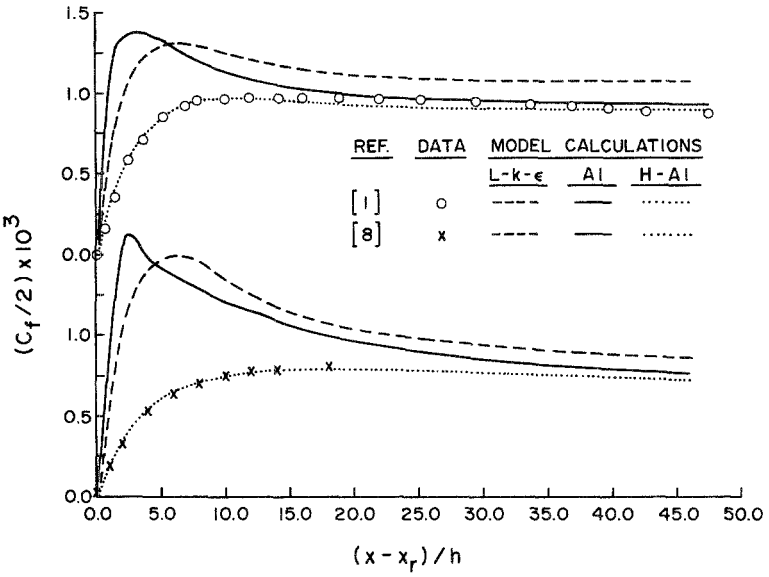

Figure 11
Comparison of c_f in the recovery region downstream of the reattachment point.

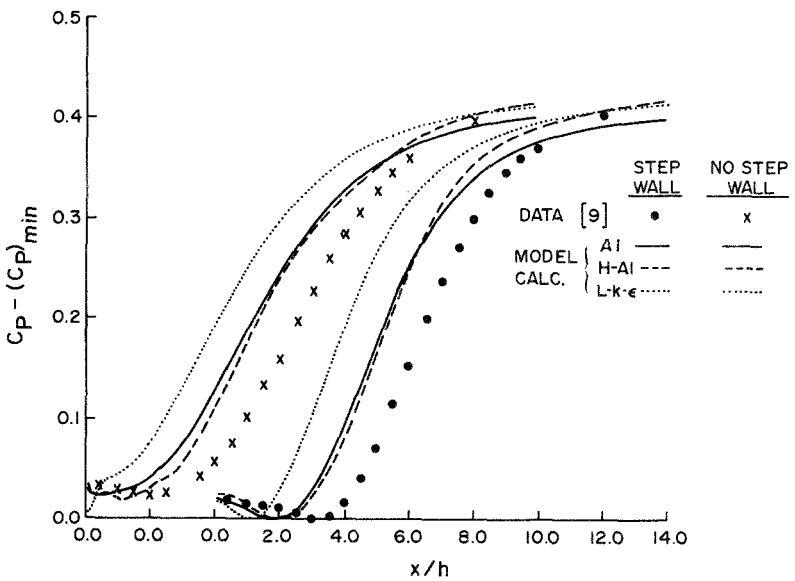

Figure 12
Comparison of the calculated and measured $C_p - (C_p)_{\min}$.

As far as the velocity field predictions are concerned, models A2 and A4 give essentially the same results; incorrect prediction of U near the wall in both the recirculation and recovery regions and along the central core (Figs. 4 and 5) and over-predictions of $\overline{uv}$ (Fig. 6) and $u' = \sqrt{\overline{u^2}}$ (Fig. 7) in the recirculation region. On the other hand, model A1 and H–A1 calculations are in excellent agreement with measurements. This comparison, therefore, shows that the benefit of mean-strain modelling in Φ_{ij} is minimal, at least for the flow over a backward-facing step. The same conclusions has also been deduced by So and Yoo [16] in their studies of simple wall shear flows. One drawback of the Rotta return-to-isotropy model for Φ_{ij} is that it gives equal distributions for the normal stresses $\overline{v^2}$ and $\overline{w^2}$, while the models of Gibson and Younis [14] and Launder et al. [11] do not. However, the simplicity of the Rotta model makes it very appealing for complex turbulent flow calculations.

Further evidence that the performance of A2 and A4 is not as good as A1 can be found in the comparison of the calculated $U = 0$ locus behind the step (Fig. 8). Of all the closure calculations presented in Fig. 8, the predictions of the $U = 0$ locus by A2 and A4 closures lie farthest away from the measured data, and are in close agreement with the predictions of the $L - k - \varepsilon$ closure. In general, the best result is given by A1 and H–A1. Once again, this shows that the benefit of mean-strain modelling in Φ_{ij} is minimal for the flow over a backward-facing step.

The predictions of c_f in the region $x/h < 3.0$ (Fig. 9) by A1, H–A1, A2 and A4 are about the same and are slightly lower than the measurements of [8]. As far as the $L - k - \varepsilon$ prediction of c_f is concerned, it is way too low compared to the other results and the measured data. This and the incorrect predictions of the velocity field preclude the $L - k - \varepsilon$ closure as a viable closure for the flow over a backward-facing step. The fact that the results of A1, H–A1, A2 and A4 are in good agreement with data and with each other in the recirculation region suggests that the near-wall flow in this region is indeed in local equilibrium and can be represented by the wall function approximation. It also shows that the low-Reynolds-number full Reynolds stress closures are capable of reproducing this behavior in the recirculation region.

All closures considered predict two $c_f = 0$ locations (Fig. 9); one very close to the step and another further downstream. This suggests the existence of a secondary recirculation near the corner of the step. A normalized stream function (ψ/ψ_0) plot based on the A1 calculation is shown in Fig. 10, and it clearly shows the presence of the secondary recirculation region. The size of this secondary recirculation region is about $h/3$ in both the x and y directions and does not seem to depend on the low-Reynolds-number closures used to calculate the flow.

Experimental measurements of Westphal et al. [8] show that c_f goes to zero at $x/h = 8$. If this is taken to be the reattachment point, then all closures fail to give a correct prediction of x_r/h. The worst performer is A2, followed by A4,

$L-k-\varepsilon$, A1 and H–A1 (Fig. 9). Since the reattachment point oscillates with time, perhaps a better prediction of x_r/h could be obtained by solving the unsteady equations. This is indeed the case, as demonstrated by the calculations of Celenligil and Mellor [6].

The predictions of c_f by all the closures considered are grossly in error compared to the measurements of [8]. This is in part due to the incorrect prediction of x_r. In order to take out the dependence on x_r, the c_f's downstream of x_r are plotted versus $(x-x_r)/h$ in Fig. 11. Shown in this plot are the measurements of [1] and [8] and the model calculations of $L-k-\varepsilon$, A1 and H – A1. The results clearly show that the behavior of c_f downstream of x_r is correctly predicted by H – A1 and is erroneously calculated by $L-k-\varepsilon$, even at a distance far downstream of x_r. On the other hand, A1's prediction of c_f is way too large in the region $0<(x-x_1)/h<15$. The reason for this discrepancy could be due to the slow response of the closure to a rapid change in streamwise pressure gradient. As shown in Fig. 12, the pressure gradient is largest around the reattachment point. The fact that the experimental measurements agree with H – A1 predictions indicates that the flow recovers quickly from the perturbation and the turbulence field in the reattached boundary layer is again in local equilibrium shortly after x_r. Apparently, this fast recovery to equilibrium flow cannot be correctly predicted by A1 and suggests that the low-Reynolds-number model of [16] should be modified to account for large pressure gradient effects. Similar remarks also apply to the $L-k-\varepsilon$ closure.

Finally, the comparison of calculated and measured $C_p-(C_p)_{\min}$ is shown in Fig. 12. Only the calculations of A1, H – A1 and $L-k-\varepsilon$ are shown together with the measurements on both the step and no step walls from [9]. The calculated curves are shifted to the left because of the under-prediction of x_r. If the predicted minimum of $C_p-(c_p)_{\min}$ is shifted to coincide with the measured minimum, then the H – A1 calculations give the best overall agreement with measurements.

7. Conclusions

The following major conclusions emerge from this study:

1. The $L-k-\varepsilon$ closure is not applicable to the flow over a backward-facing step. It gives incorrect predictions of the flow in every region downstream of the step.
2. The low-Reynolds-number turbulence closure of So and Yoo [16] reproduces the flow properties behind a backward-facing step very well in both the recirculation region and the recovery region downstream of x_r, but fails to predict correctly the c_f behavior in the region $0<(x-x_r)/h<15$.

3. The wall function approximation mimics the flow near the wall very well, especially in the region downstream of the reattachment point. Consequently, c_f in this region is predicted correctly.
4. The inability of the low-Reynolds-number full Reynolds stress closures to predict c_f correctly in the recovery region is because the near-wall model fails to account for the large pressure gradient effects in this region.
5. Of all the models considered for Φ_{ij}, the Rotta return-to-isotropy model is found to give the best overall results.
6. None of the closures considered is able to predict x_r correctly. Perhaps, the reason is the application of a steady formulation to an intrinsically unsteady problem.

Acknowledgement

The authors (RMCS, YGL and GJY) wish to acknowledge support given them by DTNSRDC, Annapolis, MD 21402, under Contract No. N00167-86-K-0075. RMCS further acknowledges support from Oak Ridge National Laboratory, Oak Ridge, Tennessee 37831, under subcontract No. 11X-57502V.

References

[1] P. Bradshaw and F. Y. F. Wong, *The reattachment and relaxation of a turbulent shear layer.* J. Fluid Mech. 52, 113–135, (1972).
[2] S. J. Kline, B. J. Cantwell and G. M. Lilley, *The 1980–81 AFOSR-HTTM-Stanford Conference on Complex Turbulent Flows: Comparison of computation and experiment* 2. Thermocsci. Div., Stanford University, Stanford, California 1982.
[3] D. W. Etheridge and P. H. Kemp, *Measurements of turbulent flow downstream of a reward-facing step.* J. Fluid Mech. *86,* 545–566 (1978).
[4] B. E. Launder and D. B. Spalding, *Mathematical Models of Turbulences.* Academic Press, London, 57–60 (1972).
[5] M. M. S. Sindir, *A numerical study of turbulence flows in backward-facing step geometries: A comparison of four models of turbulence.* Ph.D. Thesis, University of California, Davis, California 1982.
[6] M. C. Celenligil and G. I. Mellor, *Numerical solution of two-dimensional turbulent separated flows using a Reynolds stress closure model.* ASME Paper No. 85-WA/FE-5 (1985).
[7] J. Kim, S. J. Kline and J. P. Johnston, *Investigation of separation and reattachment of a turbulent shear layer: flow over a backward-facing step.* Thermosci. Div., Rept. MD-37, Stanford University, Stanford, California 1978.
[8] R. V. Westphal, J. K. Eaton and J. P. Johnston, *A new probe for measurement of velocity and wall shear stress in unsteady, reversing flow.* J. Fluid Eng. *103,* 478–482 (1981).
[9] J. K. Eaton and J. P. Johnston, *Turbulent flow reattachment: An experimental study of the flow and structure behind a backward-facing step.* Thermosci. Div., Rept. MD-39, Stanford University, Stanford, California 1980.
[10] W. H. Stevenson, H. D. Thompson and R. R. Craig, *Laser velicometer measurements in highly turbulent recirculating flows.* J. Fluid Eng. *106,* 173–180 (1984).
[11] B. E. Launder, G. J. Reece and W. Rodi, Progress in the development of a Reynolds-stress turbulence closure. J. Fluid Mech. *68,* 537–566 (1975).
[12] K. Hanjalic and B. E. Launder, *A Reynolds stress model of turbulence and its application to thin shear flows.* J. Fluid Mech. *52,* 609–638 (1972).

[13] A. N. Kolmogorov, *The local structure of turbulence in incompressible viscous fluid for very large Reynolds numbers*. C. R. Akad. Nauk. SSR *30*, 301–305 (1941).
[14] M. M. Gibson and B. A. Younis, *Calculation of swirling jets with a Reynolds stress closure*. Phys. Fluids *29*, 38–48 (1986).
[15] W. Kebede, B. E. Launder and B. A. Younis, *Large amplitude periodic pipe flow: A second moment closure study*. Proc. 5th Turbulent Shear Flows Symposium, Paper No. 16 (1985).
[16] R. M.C. So and G. J. Yoo, *On the modelling of low-Reynolds-number turbulence*. NASA CR-3294 (1986).
[17] R. M.C. So and G. J. Yoo, *Low-Reynolds-number modelling of turbulent flows with and without wall transpiration*. To appear in AJAA J. (1987).
[18] J. C. Rotta, *Statistische Theorie nichthomogener Turbulenz*. Z. für Physik *129*, 547–572; *131*, 51–77 (1951).
[19] K. Y. Chien, *Predictions of channel and boundary layer flows with a low-Reynolds-number two-equation model of turbulence*. AJAA J. *20*, 33–38 (1982).
[20] S. V. Patankar and D. B. Spalding, *A calculation procedure of heat, mass and momentum transfer in three-dimensional parabolic flows*. Int. J. Heat Mass Transfer *15*, 1787–1806 (1972).

Abstract

The complex turbulent flow behind a backward-facing step is modelled using a full Reynolds stress closure. In order to develop a closure model that can resolve the complex near-wall flow in the recirculation region and in the recovery region downstream of the reattachment point, the performance of a low and a high Reynolds number version of the full Reynolds stress closure is examined and compared. Furthermore, the effects of redistribution modelling on the calculated flow is studied by comparing the performance of three redistribution models: one return-to-isotropy model and two with mean-strain effects. The results are grid independent and show that the flow downstream of the step is best described by a low-Reynolds-number model that does not depend on the conventional wall function assumption. However, the skin friction behavior is correctly predicted by the stipulation of a wall function. Of the three redistribution models examined, the return-to-isotropy model gives results that are in excellent agreement with measurements. Finally, the calculated results are adversely affected by refining the redistribution models to include mean-strain effects.

(Received: March 7, 1987; revised: September 16, 1987)